



AXIAL CRUSHING OF SQUARE STEEL TUBES

A. A. N. Aljawi¹

1: Department of Mechanical Engineering, King Abdulaziz University,

P.O. Box 80204 Jeddah 21589 Saudi Arabia

Fax: 966-2-695-2193

E-mail: a_aljawi@hotmail.com

ABSTRACT

An experimental and a finite element method (FEM) analysis have been carried out to study the behavior of square steel tubes subjected to quasi-static and dynamic axial loadings. The non-linear finite element code ABAQUS was employed for computing and describing the deformation processes, load histories, etc. Typical histories of deformation of single steel tubes and their load-compression curves are presented. Furthermore, the good agreement in the quasi-static loading for the behavior of the FE force histories of tube with obtained experimental results is reported. The FEM analysis is extended to cover the dynamic impact loadings.

Keywords: *Energy Absorber, axial crushing, ABAQUS, square tubes, thin-walled.*

المخلص

.(ABAQUS)

1. INTRODUCTION

Nowadays, improving the crashworthiness of vehicles is considered to be one of the main concerns in traffic safety [Postlethwaite and Mills, 1970]. Shell structures are used in many engineering applications due to efficient load carrying capability relative to material volume. Of special importance in this regard is the design and development of metallic shell structures and structural components that are capable of withstanding sudden loads of large plastic deformations [Reid, 1993], [Reid et al., 1989], [Reid et al., 1984], [Reid, 1985], [Reid and Reddy, 1986], [Aljawi, and Alghamdi, 1999], [Aljawi, and Alghamdi, 2000], [Alghamdi et al., 2002], [Aljawi, 1999], [Aljawi and Ahmed, 1999], Karagiozova et al., 2000], [Langseth and Hopperstad, 1996], [Langseth et al., 1999], [Wierzbicki and Abramowicz, 1983], [Abramowicz and Jones, 1984], [Abramowicz and Wierzbicki, 1989], [Jones, 1997], [Gupta and Velmurugan, 1999], [Florence and Goodier, 1968], [Murase and Jones, 1993], [Wang et al., 1983] and [Li et al., 1994]. Familiar active plastic deformable energy absorber systems can assume several common shapes such as frusta [Aljawi, and Alghamdi, 1999], [Aljawi and Alghamdi, 2000] and [Alghamdi et al., 2002], circular tubes [Aljawi, 1999], [Aljawi and Ahmed, 1999] and Karagiozova et al., 2000], square tubes [Langseth and Hopperstad, 1996], [Langseth et al., 1999], [Wierzbicki and Abramowicz, 1983] and [Abramowicz and Jones, 1984], multicorner metal columns [Abramowicz and Wierzbicki, 1989], and rods [Gupta and Velmurugan, 1999].

Thin-walled tubular elements are used extensively in the structural crashworthiness field, so that it is important to examine various features of their dynamic response in order to predict the energy-absorbing properties of these elements and to estimate the associated crushing forces. The static and dynamic behavior of thin-walled ductile metal tubes have been studied both theoretically and experimentally in order to obtain the critical forces, types and modes of buckling and the energy absorbing properties, etc (see e.g. [Florence and Goodier, 1968],[Murase and Jones, 1993][Wang et al , 1983] and [Li et al., 1994]).

In this paper, some experimental results are reported for quasi-static axial compression of square tubes of mild steel in as-received condition. The tubes were of different widths and their lengths fixed in the experiments. Typical modes of deformation of single and parallel tubes, and the corresponding load-compression curves are presented. The manner in which the tubes collapse is compared with the results of a parallel finite element study. The good agreement that is obtained between the experimental and finite element studies in quasi-static loading is taken as an encouragement to extend the study to dynamic impact loadings, despite the lack of an experimental set-up for this. Strain rate effects are also considered when discussing the energy absorbing properties of the tubes.

2. EXPERIMENT WORK AND FINITE ELEMENT MODELING

In this section both the experimental procedures as well as the finite element modeling will be discussed.

2.1. Experimental

Mild steel square tubes employed in the test were of three different sizes. The mean width of the tubes are 30.0, 50.0 and 60.0 mm and wall thickness and length were kept at 1.5 mm and 150.0 mm, respectively. Thus the width to thickness, W/t , ratio of these tubes varied from 20.0 to 40.0. The length to width, L/W , ratios were varied from 5.0 to 2.5. An Instron Universal testing machine was used to perform all quasi-static tests. The tubes were subjected to axial compression. The speed of testing was generally 200mm/min, and load-displacement curves in the tests were obtained on the automatic chart recorder of the machine.

2.2. Finite element modeling

Many structural dynamics have been modeled using finite element method (FEM) [Aljawi and Alghamdi, 1999], [Alghamdi and Alghamdi, 2000], [Alghamdi et al., 2002], [Aljawi, 2000], [Aljawi and Ahmed, 1999] and [Karagiozova et al., 2000], [Langseth et al., 1999], [Wierzbicki and Abramowicz, 1983], [Abramowicz and Jones, 1984], [Abramowicz and Wierzbicki, 1989], [Jones, 1997], [Gupta and Velmurugan, 1999], [Florence and Goodier, 1968], [Murase and Jones, 1993], [Wang et al., 1983], [Li et al., 1994] and [HKS, Inc, 1998]. In this study, ABAQUS/Explicit and Implicit FEM code (version 5.8) is employed to investigate the modes of deformation of tubes under quasi-static and dynamic loading conditions with large strain analysis. Full 3-dimensional discretized model shown in Fig. 1 is considered. The model consists of three parts. These are a) the tube, b) the rigid surfaces representing the crushing surfaces, and c) the mass element, representing the hammer striker. Four noded shell elements (S4R) are used in the discretized model. The rigid surfaces are modeled with a four-noded rigid element (R3D4). Several mesh size simulation were carried out to determine the proper mesh density, and an element size of 2.5×2.5 was sufficient giving a total of 2880 elements in the tube of 30.0 mm width.

Constraints were imposed on reference nodes, located at the tip of the upper and the lower rigid surfaces. It is to be noted that the upper rigid surface can carry the relatively large mass element, representing the striker, and generates the impact loading of the tube. Note that for the quasi-static case no mass is considered for the striker. In order to prevent sliding at the proximal ends, all the bottom tube nodes were attached with the bottom of the rigid body. A coefficient of friction of $\mu=0.15$, was incorporated between the tube surfaces, using the surface interaction.

Material properties of the model were modeled as elasto-plastic materials, using isotropic plasticity, standard von Mises yield criterion and an associated flow rule; with yield strength $\sigma_y=280$.MPa, mass density, $\rho=7830$. Kg/m³, Poisson's ratio, $\nu=0.3$, Modulus of Elasticity, $E=207$.Gpa

In this model analysis, in order to obtain a smooth postbuckling response of the deformed tube; the first 10 buckling modes were obtained by running an eigenvalue buckling analysis of the tube using ABAQUS/Standard. Then, the *IMPERFECTION option in ABAQUS/Explicit was introduced to read the buckling modes, and to perturb the nodal coordinates [HKS, Inc, 1998].

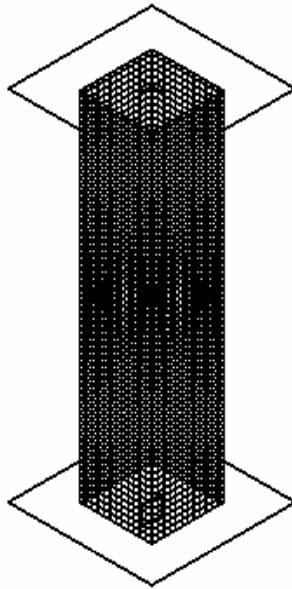


Fig.1 Discretized 3-dimensional model

The numerical simulation was performed on a Pentium IV PC 1.6 GHz and a typical quasi-static case took 30-40h. Unless otherwise stated, and in order to reduce the computational costs, most of the analysis were performed on the 30.0 mm tube width.

3. RESULTS AND DISCUSSION

In this section, detailed outcomes of the experimental work and results of the finite element analysis are presented for quasi-static as well as for dynamic loadings.

3.1. Quasi-static loading

3.1.1. Numerical simulation

As stated earlier in order to initiate the symmetric deformation modes, triggering or imperfections were introduced in the analysis of ABAQUS/Explicit using the first 10 buckling modes which were obtained by running an eigenvalue buckling analysis of the tube using ABAQUS/Standard.

Fig. 2 demonstrates the good agreement and similarity between the final deformed shape of the tube which has been crushed experimentally, Fig. 2(a), and the shape predicted 3-dimensional ABAQUS models, Fig. 2(b) and 2(c). Fig. 2(b) is for mesh size of 1.5×1.5 , and Fig. 2(c) is for mesh size 2.5×2.5 . It is important to note that ABAQUS/Explicit includes the thickness of the shell in the contact calculations, the regions that are in contact appearing with a slight gap between contacting regions. Fig. 2 shows that when the specimens in the analyses are fully compressed, the number of lobes obtained during the experimental program, are well predicted by the numerical analyses with a imperfections.

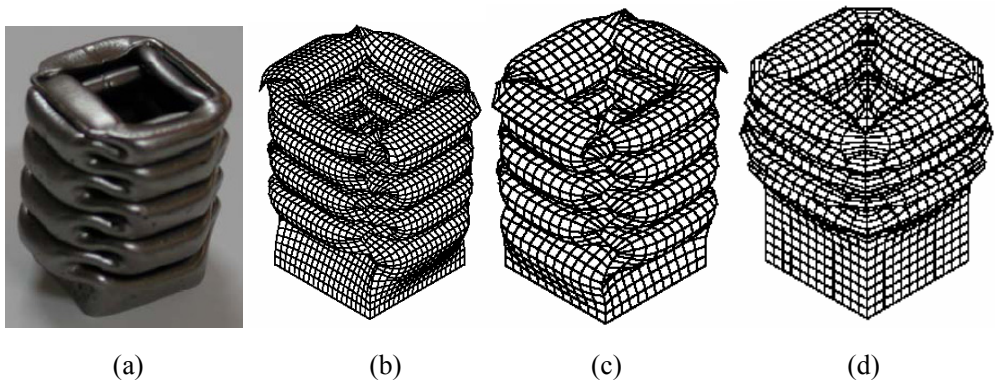


Fig. 2. Comparison of deformed tubes between; (a) experimental, and ABAQUS (b) perturbed fine mesh, (c) perturbed medium mesh, (d) unperturbed medium mesh.

The importance of the perturbing mesh can clearly be observed from Fig. 2(d) prior to performing a postbuckling analysis. The final deformed mesh of an analysis that includes no initial imperfections, shown in Fig. 2(d), deforms into folds that are clearly not physically correct. On the other hand small imperfections introduced in the perturbed mesh are sufficient to smoothly deform the mesh in a symmetric mode.

3.1.2. Load-displacement curves

Typical load-compression curves are shown in Figs. 3 and 4, as measured experimentally and also predicted by ABAQUS. Fig.3 is for tube width of 30.0 mm, while Fig. 4 is for tube width of 60.0 mm. The progressive deformation steps predicted by ABAQUS to form the folds along the tube surface at successively increasing displacements are also shown in Fig. 3. These steps are selected at 8 steps to correspond to some local maxima and minima of the curve. Good agreement and almost full conformance can clearly be observed for the peak force and the number of folds. However, both figures reveal that the first experimental peak load observed to be somewhat shifted relative to the predicted values. This may be attributed to the initial post-buckling behavior of the tube, which occurs at large plastic strains. The effect of increasing the width of the tube from 30.0 mm to 60.0 mm shown in Fig. 4. shows that an increase in the tube width tends to increase the crushing load and to decrease the number of tube folds.

3.1.3. Deformation processes

It may be observed from Figs. 3 and 4 that, a complete description of the collapse process involves several stages. That is, when compression starts, the first fold usually tends to form outwards, from the two opposite sides of the tube, and inwards from the other two. The folds starts with a load peak rises rapidly higher than the other peaks, until the plate tube sides collapse. The load then decreases rapidly to the first local minimum, in which the first flattening outward and inward folds are fully developed. That is, folding of the walls in the vicinity of one end of the tube started. Folding mode was symmetric about the neutral axis of the tube cross-section, i.e., two opposite sides folded inward and the other two outward.

The second increase in the load can be observed, after the first folding of the walls ended; i.e., contact of the walls started leading to forming of the second folding of adjacent walls. Then, the second drop of the load occurred again indicating the second folding of the walls. Thus, the load drops when new folding started, and rises when the walls come into contact. This process is repeated until the folding ended the tube is completely squashed in which the crushed tube behaves as a rigid body.

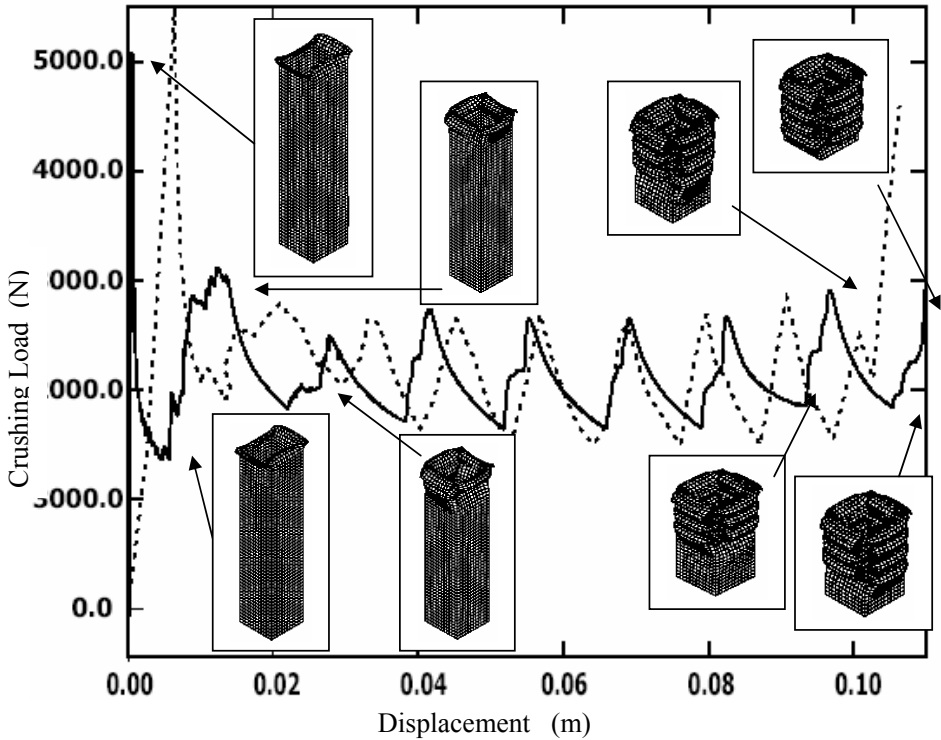


Fig. 3. Experimental (....), and ABAQUS (—), load-displacement results, and quasi-static development of forming folds along the tube at 8 axial displacements: 1) 4.4 mm, 2) 6.0 mm, 3) 13.2 mm, 4) 22.0 mm, 5) 92.2 mm, 6) 96.8 mm, 7) 105.6 mm, and 8) 110.0 mm, for tube width 30. mm, and length of 150. mm

3.1.4. Numerical results

Wierzbicki and Abramowicz [Wierzbicki and Abramowicz, 1983] analyzed the crushing of thin-walled multicorner structures made from plate elements, by considering stationary plastic hinges and narrow toroidal regions of circumferential stretching and bending which travel through the structure. As a special case of the multicorner column, the mean crushing load (P_m) for the symmetrical collapse mode of a square tube made of rigid-plastic material takes the form,

$$P_m = 9.56\sigma_0 t^{5/3} W^{1/3} \quad (1)$$

where, σ_0 is the yield stress, W is the width of the square tube and t is the column thickness. By assuming an arbitrary angle between the adjacent plates of the structure, Abramowicz and Wierzbicki [Abramowicz and Jones, 1984] predicted an improved

model previously defined in [Abramowicz and Wierzbicki, 1989] for the average static crushing force for asymmetric collapse of a square tube to as,

$$P_m = 13.06\sigma_0 t^{5/3} W^{1/3} \tag{2}$$

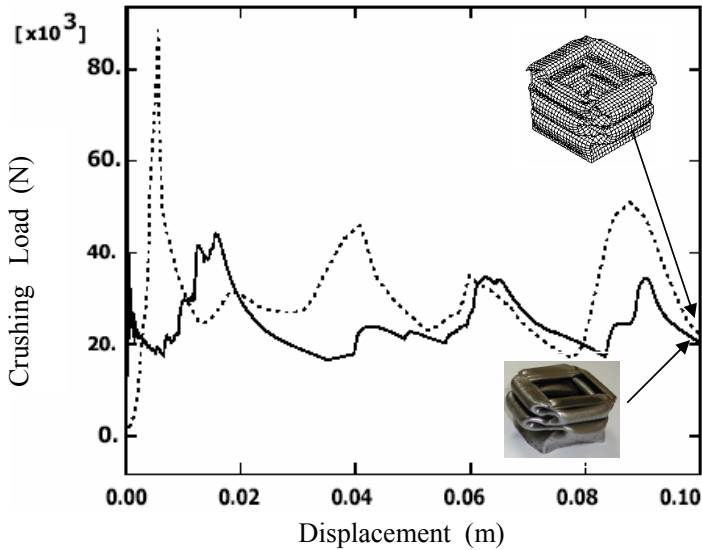


Fig. 4. Experimental (....), and ABAQUS (—), load-displacement results, and final deformed square tubes of tube width 60. mm, and length of 150. mm

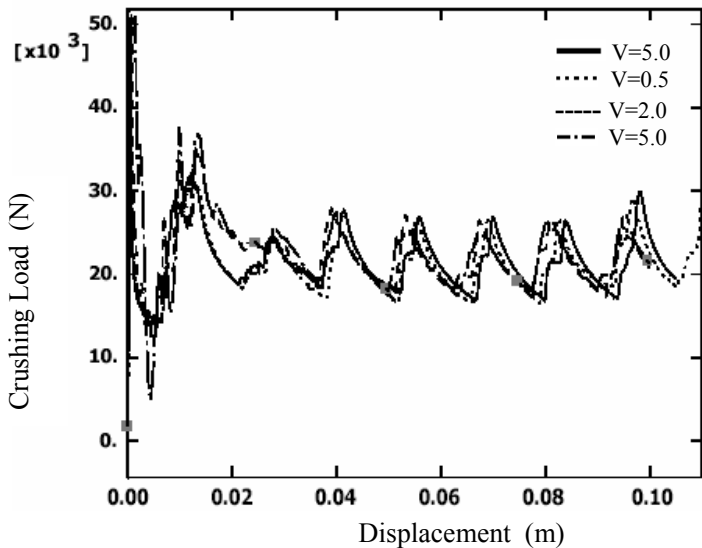


Fig. 5. ABAQUS load-displacement curve for square tube compressed at different constant axial velocities; $V=0.25, 0.5, 2.0,$ and 5.0 m/s.

Note that Eq. (2) takes into account the average flow stress and it was found to be in good agreement with experimental results. Using Eq. (2), the average load can be found to be 22.333 KN. However, from Fig. 3 the experimental and FEM average loads for the crushing length of 106.3 mm are: 22.164 KN, and 21.33 KN, respectively. It can clearly be shown that there is a good agreement between the theoretical and both the experimental and FE analysis.

3.1.5. Compression rate effect

Numerical results concerning the important effect of relatively high-speed rate on the load-displacement and deformed shape are shown in Figs. 5 and 6. Fig. 5 demonstrates the load-displacement curves for the tubes which are crushed at different constant axial velocities; $V=0.25, 0.5, 2.0,$ and 5.0 m/s. It can be observed from this figure that all velocities reveal almost similar initial peak loads. However, higher velocities tend to shift other peak loads to the right signaling different shape of deformations, i.e., no symmetric modes but with similar number of outward and inward extensional lobes or folds, as shown in Fig. 6. Whereas lower compression rates will give both load-displacement as well as deformed shapes closer to the experimental results. Thus, the energy-absorbing characteristics of elastic-plastic tubular elements are often associated with folding mechanisms of deformation, which form progressively.

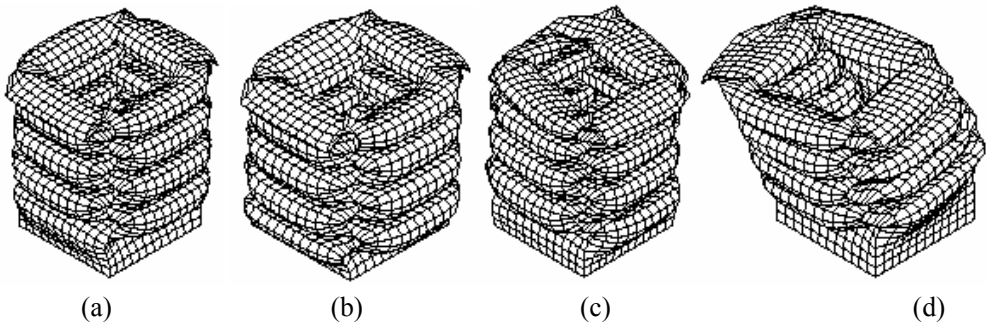


Fig. 6. Final deformed square tubes crushed at constant axial velocity, V ; a)0.25 m/s, b)0.5 m/s, c)2.0 m/s, and d)5.0 m/s.

3.2. Parallel tubes

Measured load-displacement curves for tubes staggered in parallel is shown in Fig. 7 which were compressed axially singly, in two, and in three tubes. It is clear that load capacity increases with the increase in number of tubes. However, although not shown here, in the quasi-static condition, experimental observations indicate that load-carrying

capacity of tubes in parallel under axial compression is apparently not equal to the sum of the load-carrying capacities of each tube acting in the absence of the other. No change can be observed however, between tubes that are deformed in parallel and the one obtained for a single tube. Photographs of the final experimental crushed tubes staggered in parallel of width sizes 30.0 and 60.0 mm are shown in Figs. 8(a)-8(c).

3.3. Inertial effects

The variation, with time, of the dynamic crushing load, and kinetic energy, of the square tube when subjected to equal impact energies, resulting from different combinations of striking mass and initial velocities, are shown in Figs. 9 (a) and (b), respectively. As it would be expected, all of the curves indicate that, as kinetic energy decreases with time, most of the energy is being transferred to the tube, and consumed for deformation and plastic work dissipation. Then kinetic energy tends to zero where no energy is available for the striker. For lower velocities, the contact time of the striker with the tube is longer than the higher initial impact velocities; indicating that the crushing distance decreases with the increase in initial impact velocities, implying that more energy is required for the complete folding of the tube. Although not shown it is found that that the average crushing force (which is obtained by dividing the energy by the crushing distance) increases with the increase in impact velocities and a decrease of the impact mass. This latter phenomenon seems to be largely due to inertia effects, since more energy is absorbed by the tube during initial buckling when higher impact velocities are used.

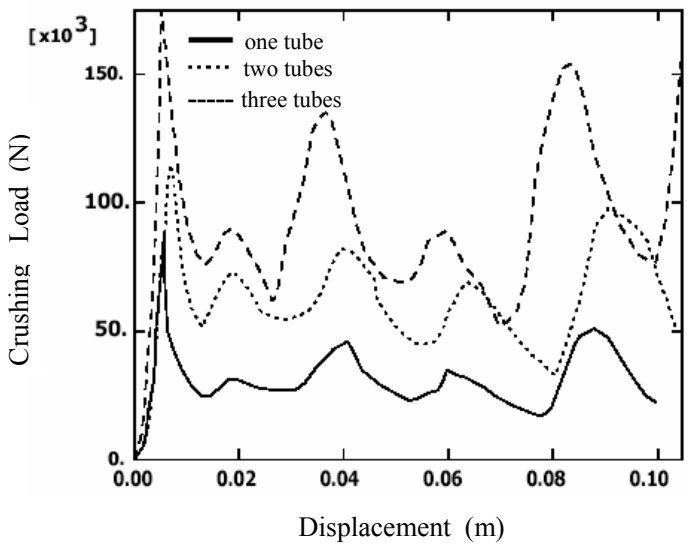


Fig. 7. Measured load-displacement curves for axially compressed parallel square steel tubes, one (—), two (....), and three tubes (- - -), of tube width 60.0 mm and length 150. mm

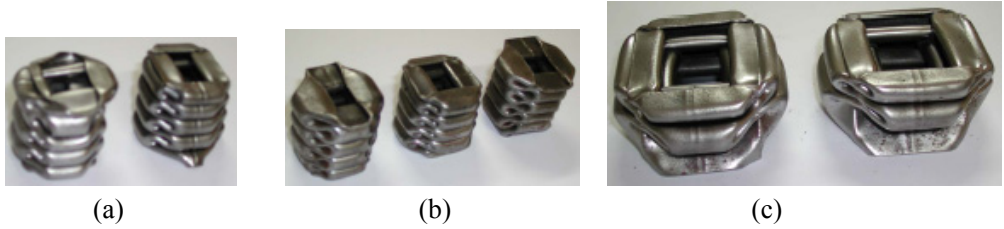


Fig. 8. Photographs of final deformed crushed tubes staggered in parallel, a) two, b) three, and c) two, square tubes.

The final deformed shape of the tube when subjected to equal impact energies with different combinations of mass and initial velocities of the striker is shown in Fig. 10. It is evident from Figs. 10(a)-10(d) that a quasi-static load as well as low impact velocity cause a tube to collapse by a progressive folding process for which the deformations occur locally, while high velocity impacts cause deformations to develop over the entire length of the tube due to inertia effects. Fig. 10 also shows the importance of using the full 3D-model, in which different shape of mode deformations (that is, symmetric and non symmetric modes of deformation with different number of inward and outward extensional lobes or folds) can occur for different combinations of striking mass and impact velocities.

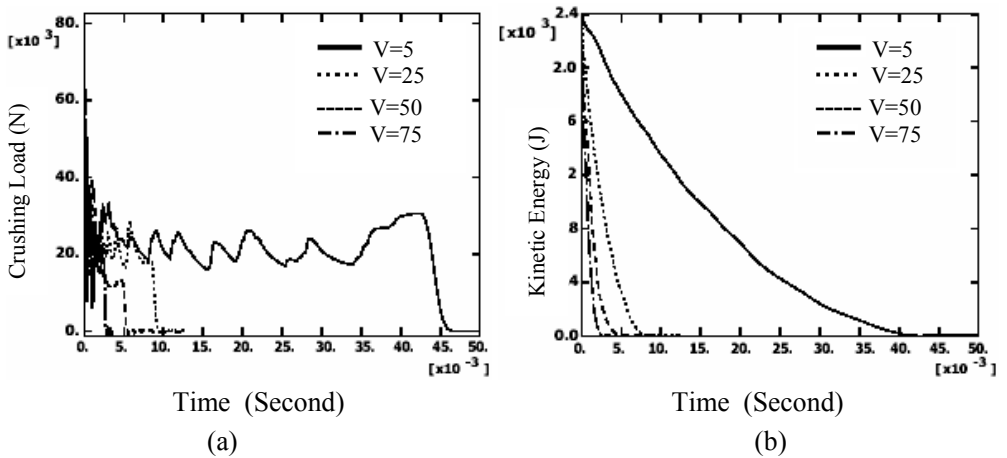


Fig. 9. Effect of impact energy of 2.4 KJ with different combinations of striking mass and impact velocities (a) crushing load, (b) kinetic energy.

Figs. 11(a) and 11(b) show the results for the case when, the impact velocity of the striker was kept constant at 25 m/s, and the mass of the striker is kept constant at 25.0 kg, respectively. It is evident from Fig. 11(a), that no significant changes can be observed in

the load-displacement curves when the mass of the striker is increased from 5-20 kg. However, Fig 11(b) reveals higher peak loads when the velocity is increased form 10-20 m/s. It is worth noting that, an increase in axial displacement can be noticed in both Figs. 11(a) and 11(b) with the increase of the mass and the velocity of the striker, this is due to the increase of the initial impact energy. Although not shown different deformation shape were found similar to those shown in Fig. 10.

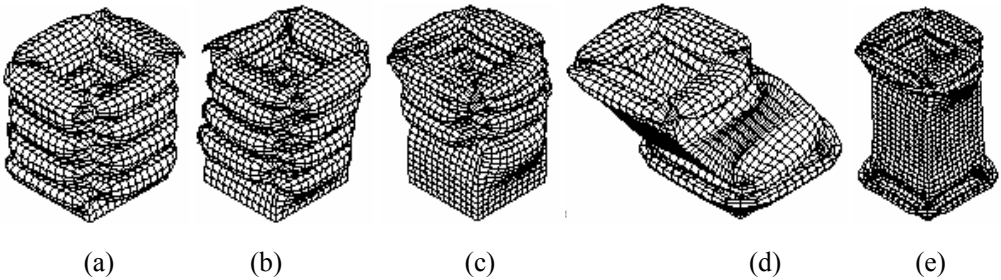


Fig. 10. Effect of impact energy of 2.4 KJ with different combinations of striking mass and impact velocities, final deformed shape at: (a)quasi-static, b) $V=5.0$ m/s and $m=192.0$ kg, c) $V=25.0$ m/s, and $m=7.68$ kg, d) $V=50.0$ m/s and $m=1.92$ kg, e) $V=75.0$ m/s and $m=0.85333$ kg.

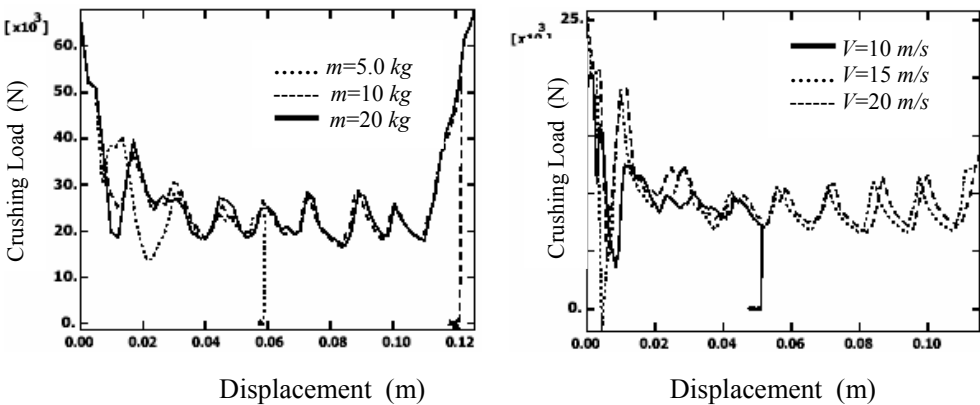


Fig. 11. Load displacement curves for square tubes, for cases of; a) constant impact velocity, $V=25.0$ m/s, b)constant striker mass, $m=25$ kg.

3.4. Rectangular tubes

The effect of decreasing or increasing the width of square tubes is shown in Fig. 12. In fact figures 12(a) and (b) show the crushing load and the energy dissipated due to plastic deformation against displacement. Results for square tubes (defined by L30) are also presented for comparisons. Fig. 12 reveals that an increase in the size of two sides of square tubes from 30.0 mm(L30) to 36.0mm (L36) tends to increase the peak loads and consequently the energy dissipated due to plastic deformation. Whereas the decrease in the size of two sides of square tubes from 30.0 mm(L30) to 24.0mm (L24) tends to decrease the peak loads and consequently the energy dissipated due to plastic deformation. Note that no change was found in the number of folds.

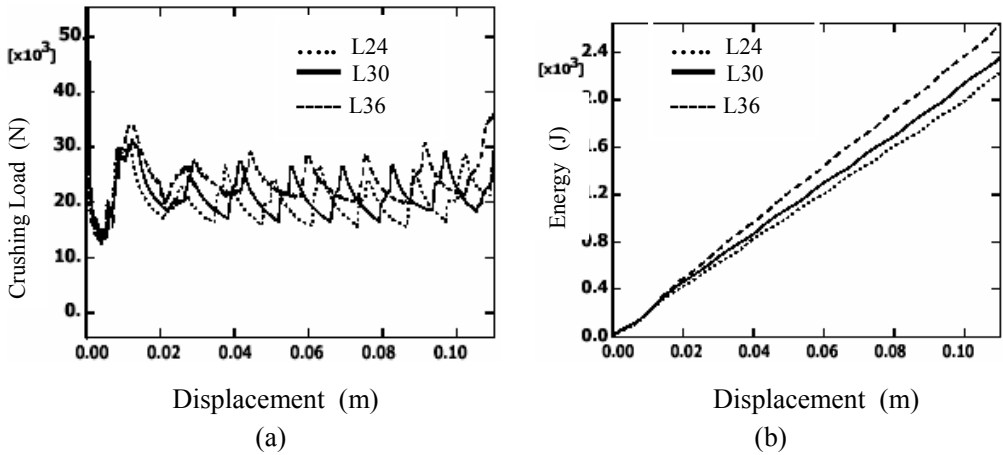


Fig. 12 (a) Load-displacement curve, and (b) energy dissipated due to plastic deformation, of rectangular tubes.

3.5. Strain rate effect

Experimental findings [Aljawi and Ahmed, 1999]and [Karagiozova et al., 2000] indicate that structures subjected to an in-plane mass impact, even within the range of low velocity impacts, are highly sensitive to strain rate and inertia effects, and they are both velocity and mass sensitive. The strain rate can be expressed by the Cowper-Symonds [Symonds, 1965] empirical power law:

$$\bar{\sigma}(\bar{\epsilon}^p) = \sigma_s(\bar{\epsilon}^p) \left[1 + \left(\frac{\dot{\bar{\epsilon}}}{D} \right)^{\frac{1}{p}} \right]$$

Where, σ_0 is the quasi-static yield stress, σ_d denotes the dynamic yield stress, $\dot{\epsilon}$ is the strain rate, and D and P are material constants. The values of $D=40.5 \text{ s}^{-1}$ and $p=5$ are basically adopted for mild steel. It was pointed out in [Karagiozova et al., 2000] that for mild steel, $D=300 \text{ s}^{-1}$ and $p=2.5$ yield reasonable results that agree well with experimental findings. In the present study, for $D=40.5 \text{ s}^{-1}$ and $p=5$, and also for $D=300 \text{ s}^{-1}$ and $p=2.5$, an increase was observed in the maximum energy required for complete crushing. However, no change was observed for energy levels during the progressive buckling phenomenon.

4. CONCLUDING REMARKS

The crushing behavior of square mild steel tubes of W/t ranging between 20 and 40 is studied experimentally and by the use of the nonlinear finite element code ABAQUS, when subjected to quasi-static and impact dynamic axial loading. Both ABAQUS explicit and implicit FEM code (version 5.8) are employed to investigate the modes of deformation, utilizing a 3-dimensional discretized model. Typical histories of deformation of single as well as parallel steel tubes and their load-compression curves are presented. Good agreement is reported between the FEM force histories of tubes with those obtained by experimental results for quasi-static loading. The FEM analysis is further extended to cover dynamic impact loading. Strain rate effects are also considered when discussing the energy absorbing properties of the tubes.

5. ACKNOWLEDGMENT

The author would like to express his thanks and appreciation to Professor M. Akyurt for his valuable comments and help during the preparation of this manuscript.

REFERENCES

1. Abramowicz, W, Jones, N., 1984, "Dynamic axial crushing of square tubes," *Int J Impact Engng*, 2(2), pp 179–208.
2. Abramowicz, W., and Wierzbicki, T., 1989, "Axial Crushing of Multicorner Sheet Metal Columns," *J Appl Mech*, 56(1), pp 113–20.
3. Alghamdi., A. A. A., Aljawi, A.A. N, and Abu-Mansour, T. M., 2002, "Modes of Axial Collapse of Unconstrained Capped Frusta," *Int. J. of Mech. Sci.* Accepted
4. Aljawi, A A N, Alghamdi, A A A., 1999, "Investigation of Axially Compressed Frusta as Impact Energy Absorbers," *Proceedings, Computational Methods in Contact Mechanics IV*, (GAUL, L, BERBBIA A A, Editors), pp 431-443, WIT Press, Southampton,.

5. Aljawi, A A N, and Alghamdi, A A A., 2000, "Inversion of Frusta as Impact Energy Absorbers," *In: Current Advances In Mechanical Design and Production VII*, (HASSAN, M F, And MEGAHED, S. M, Editors), pp511-519, New York:Pergamon.
6. Aljawi, A.A.N., and Ahmed, M.H.M., 1999, "Finite Element Analysis of the Axial Compression of Tubes," *Alexandria Eng. Journal.*, 38(6), pp. A445-A452.
7. Aljawi, A.A.N., 2000, "Finite Element and Experimental Analysis of Axially Compressed Plastic Tubes," *European. J. Mech. &Env. Eng. M*, 45(1), pp 3-10.
8. Florence, A. L., and Goodier, J. N., 1968, "Dynamic plastic buckling of cylindrical shells in sustained axial compressive flow," *J Appl Mech*, 35(1), pp 80-6.
9. Gupta, N. K., and Velmurugan, R., 1999, "Axial compression of empty and foam filled composite conical shells," *J Compos Mater*, 33(6), pp 567-591.
10. HKS, Inc, 1998, *ABAQUS/Explicit User's Manual, Theory and examples manual and post manual*, Version 5.8, Explicit.
11. Jones, N., 1997, *Structural impact*. Cambridge: Cambridge University Press, 1989, Paperback ed.
12. Karagiozova, D., Alves, M., and Jones, N., 2000,"Inertia Effects in Axisymmetrically Deformed Cylindrical shells under Axial Impact," *Int. J. Impact Engng.*, 24, pp. 1083-1115.
13. Langseth, M, and Hopperstad, OS., 1996, "Static and Dynamic Axial Crushing of Square Thin-Walled Aluminium Extrusions", *Int J Impact Engng*, 18(7-8), pp 949-68.
14. Langseth, M, Hopperstad, OS, and Brstad, T, 1999, "Crashworthiness of Aluminium extrusions:Validation of Numerical Simulation, Effect of Mass Ratio and Impact Velocity," *Int J Impact Engng*, 22, pp 829-854.
15. Li, M., Wang, R., and Han, M., 1994, "An experimental investigation of the dynamic axial buckling of cylindrical shells using a Kolsky bar," *Acta Mech Sinica*,10, pp260-66.
16. Murase, K., and Jones, N., 1993, "The variation of modes in the dynamic axial plastic buckling of circular tubes," Proceedings, (GUPTA, N. K, Editor). *Plasticity and impact mechanics.*, pp. 222-237, New Delhi: Wiley Eastern Limited,
17. Postlethwaite, H.E. and Mills, B., 1970, "Use of Collapsible Structural Elements as Impact Isolators, with Special references to Automotive Application," *Journal of Strain Analysis*, 5(1),pp 58-73.
18. Reid, S. R, Reddy, T. Y., and Peng, C., 1989, "Dynamic Compression of Cellular Structures and Materials in Structural Crashworthiness and Failure (edited by N. Jones and T. Wierzbicki). J. Wiley, New York.
19. Reid, S. R., 1985, "Metal Tube as Impact Energy Absorbers," *Metal Forming Impact Mechanics*, pp 249-269.
20. Reid, S. R., 1993, "Plastic Deformation Mechanisms in Axially Compressed Metal Tubes Used as Impact Energy Absorbers," *Int. J. Mech. Sci*, 35(12),pp 1035-1052.
21. Reid, S. R., and Reddy, T. Y., 1986, "Static and Dynamic Crushing of Tapered Sheet Metal Tubes of Rectangular Cross-Section," *Int. J. of Mech. Sci*, 28(9), pp 623-637.

22. Reid, S. R., Austin, C. D., and Smith, R., 1984, "Tabular Rings as Impact Energy Absorbers," *Structural Impact and Crashworthiness*, 2, pp 555-563.
23. Symonds, P. S., 1965, "Viscoplastic Behavior in response of Structures to Dynamic Loading," *Behavior of Materials Under Dynamic Loading* (N. J., Huffington, N. J., Editor), pp 106-124, SME, New York.
24. Wang, R., Han, M., Huang, Z., and Yan, Q., 1983, "An experimental study on the dynamic axial plastic buckling of a cylindrical shell," *Int J Impact Engng*, 1, pp 249-56.
25. Wierzbicki, T., and Abramowicz, W., 1983, "On the crushing mechanics of thin-walled structures," *J Appl Mech*, 50(4), pp 727-34.